Electronic Structure of a Novel Class of Nanoporous Materials

F. Starrost,[1] E. E. Krasovskii,[1] W. Schattke,[1] J. Jockel,[2] U. Simon,[2] X. Wang,[3] and F. Liebau[3]
[1]*Institut für Theoretische Physik, Christian-Albrechts-Universität Kiel, Physikzentrum, Leibnizstraße 15, D-24098 Kiel, Germany*
[2]*Institut für Anorganische Chemie-FB 8, Universität-GH Essen, Schützenbahn 70, D-45127 Essen, Germany*
[3]*Mineralogisch-Petrographisches Institut und Museum, Christian-Albrechts-Universität Kiel, Olshausenstraße 40-60, D-24098 Kiel, Germany*
(Received 6 November 1997)

The electronic structure of crystals from the cetineite family, a promising new nanoporous material, is theoretically investigated for the first time on an *ab initio* basis. The trend experimentally observed in the optical gaps' dependence on the chemical composition is explained. [S0031-9007(98)05777-9]

PACS numbers: 71.15.Ap, 71.20.−b, 71.20.Ps, 78.20.−e

The chemical preparation of nanostructured materials has become an important field from the scientific as well as from the technical point of view. On the one hand, various chemical routes have been developed to synthesize well defined metal or semiconductor nanoparticles of a few up to tens of nanometers [1,2], in which quantum size effects as well as charging effects occur, giving rise to various electro-optical [3] or microelectronic applications [4–7]. On the other hand, attempts have been made to obtain semiconductor or metallic solids with definite void spaces, like in zeolites, which may be regarded as so-called quantum-anti-dot lattices [8,9]. With the family of cetineite-type oxoselenoantimonates III, for which synthesizing methods have been developed [10–12], a novel class of nanomaterials has become accessible. Recently it has been found that these compounds show a pronounced photoconductivity [12]. Thus, a wide field for potential application has been opened by their electrical properties which up to now are unique in the domain of nanoporous crystalline solids.

On the theoretical side little is known about the electronic structure of these materials beyond the general picture of chemical bonds, especially no *ab initio* calculations on the electronic structure and the optical properties have been done, to the authors' knowledge. Even for the class of zeolites, which have been most common nanoporous materials already for a long time only few *ab initio* calculations exist because of the complexity of the systems [13]. The considered compounds have the general formula $A_6[Sb_{12}O_{18}][SbX_3]_2 \cdot (6 - mx - y)H_2O \cdot x[B^{m+}(OH^-)_m] \cdot y\square$ ($A = Na^+$, K^+, Rb^+; $X = S^{2-}$; Se^{2-}; $B = Na^+$, Sb^{3+}; $\square$ may stand for an unoccupied lattice site). The crystal structures, Fig. 1, have space group symmetry $P6_3$ or $P6_3/m$ [10,11]. Tubes of composition $[Sb_{12}O_{18}]$ are formed by linking $[SbO_3]$ pyramids. The lone electron pairs of their Sb(2) and Sb(3) atoms are perpendicular to the tube walls. The tube arrangement can be described as an hexagonal rod packing. Single $[Sb(1)X_3]^{3-}$ pyramids are located between the tubes. Their lone pairs are oriented parallel to the tube axes. The interior of the tubes, whose free diameter is approximately 7 Å, may be occupied by chains of face-sharing $[H_2O]_6$ octahedra or by $[(Na,Sb),(OH,H_2O)_6]$ octahedra extended along the tubes.

The arrangement of electroneutral $[Sb_{12}O_{18}]$ tubes should be held together by ionic bonds between the $[SbX_3]^{3-}$ pyramids and the A^+ cations lining the tube walls, and by additional weaker secondary bonds between every second Sb atom of the tubes [Sb(2) in Fig. 1] and the X atoms of the $[SbX_3]^{3-}$ pyramids.

Thus, there arises a most fascinating combination of structural and physical properties. The cetineite-type compounds may act like molecular sieves such as the zeolites but in contrast they reveal an optical gap in the visible range and nonzero electronic conductivity. At first glance the latter may be attributed to the electron lone pair of Sb^{3+} in the $[SbX_3]$ pyramids by structure-chemical arguments.

A lot of questions arise as to the electronic structure, specifically about the extent and the neighborhood of the electronic gap being a key to the understanding of the binding mechanism and the conductivity.

In this contribution we concentrate on the calculation and a first interpretation of the results to clarify the orbital composition near the gap and the observed optical properties in connection with the electronic conductivity. Especially, we will focus on the experimentally observed chemical trend in the optical gaps and its theoretical counterpart.

The numerical computation follows the linear augmented plane wave (LAPW) procedure [14] and yields density of states (DOS), band structure, and dielectric function ε for members of the cetineite family with $A =$ K, Na and $X =$ S, Se. We use the abbreviation $(A;X)$ for $A_6[Sb_{12}O_{18}][SbX_3]_2$ in the course of our studies. The channel filling ions B^{m+} and water molecules (or hydroxyl groups OH^-) are considered to be strongly disordered and have been discarded in the calculation because of their minor importance and the computational burden. An effect on the electrical and optical properties has not been detected in experimentally investigating different samples. Especially, an ionic conductivity, perhaps by water and/or B^{m+}, has been excluded via impedance measurements [12]. In addition to the real

 0031-9007/98/80(15)/3316(4)$15.00

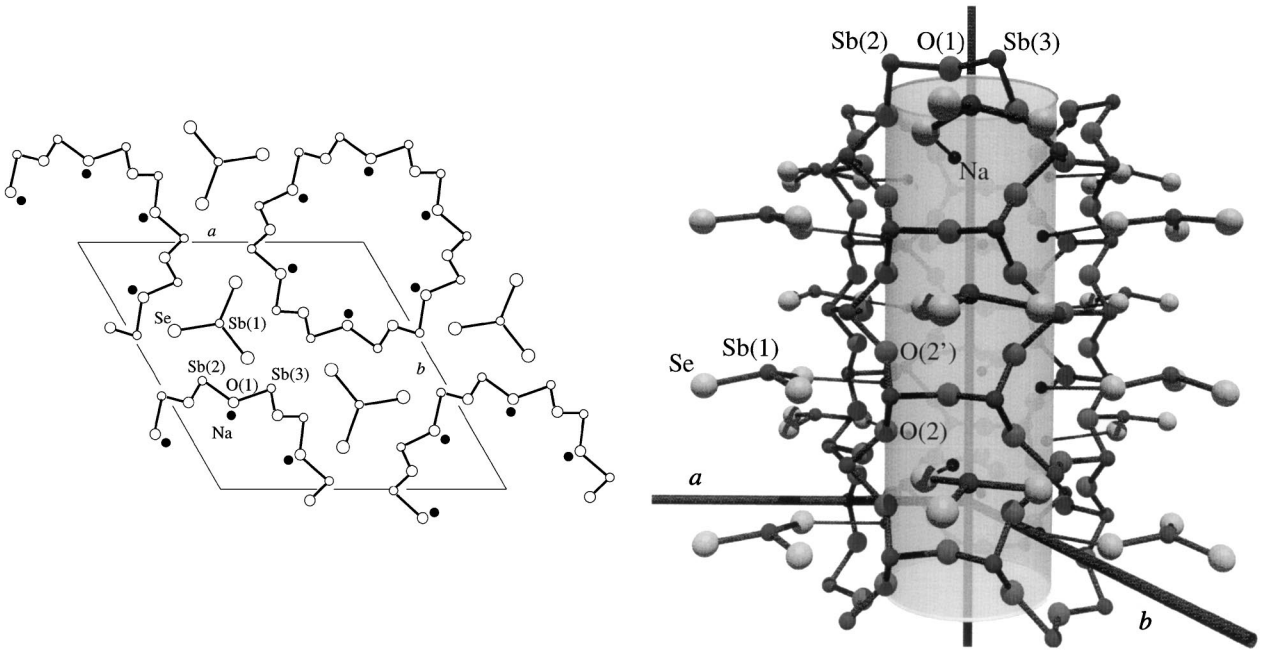

FIG. 1. Structure of cetineite (Na;Se): projection onto the ab plane (left), perspective view of one tube (right), $a = b$ in the $P6_3$ space group; the shaded cylinder is for the illustration of the three-dimensional view; the channel filling ions and water molecules are left out in the plot as well as in the calculations; the Na-Se ionic binding is sketched, too.

crystals, systems are considered, where only some of the molecular constituents are taken into account, forming fictitious crystals. This provides specific information as to which orbitals contribute to the bands and the binding. Aspherical corrections to the muffin tin approximation are introduced finally by adding an empty sphere within the tubes. We have self-consistently calculated the potential for the four crystals with 44 atoms per unit cell and an empty sphere centered in the tube. The atomic coordinates of (K;S) [15] were used for the unit cell of all compounds because of only small variations in their values. The number of LAPW basis functions was slightly less than 700 in all cases so that $|\vec{G}_{\max}|S_{\min}$ was slightly below three, where S is the radius of the muffin tin spheres. In the unit cell there are eight different inequivalent types of atoms. The lattice constants used for (K;Se), (Na;Se), (K;S), and (Na;S) are $a = 14.595$, 14.423, 14.318, and 14.152 Å and $c = 5.617$, 5.565, 5.633, and 5.576 Å, respectively. The $2 \times 2 \times 1$ superstructure of (K;Se) [15] has not been taken into account. Iterating to self-consistency, the electronic properties were calculated for 18 points in the irreducible Brillouin zone (BZ) which is one third the size of the full BZ.

As a prototype for these compounds the band structure of (Na;Se) is displayed in Fig. 2 along the symmetry lines of the hexagonal BZ. The stronger dispersion parallel to the c axis, especially along the ΓA direction, and the weaker one perpendicular to it is remarkable. It shows the stronger binding along the tubes which may be seen as stabilizing the tubular structure whereas the binding between the tubes is weaker. The main contribution to the binding within the tube walls occurs, however, via Sb(2)- [Sb(3)-] oxygen p bonds. The Sb s orbitals are involved in the energy range -13 to -11 eV whereas the p orbitals are found between -9 and -4 eV.

The fundamental gap is framed by states which, to a significant degree, are made up of orbitals belonging to the Sb and chalcogen atoms of the outer $[SbX_3]^{3-}$ pyramids, thereby reminding one of a lone pair state at the antimony atom, but being here dominated by a d and not p character; see Fig. 3. The antimony atoms of the wall pyramids carry a sp character as is usually assumed for a lone pair state

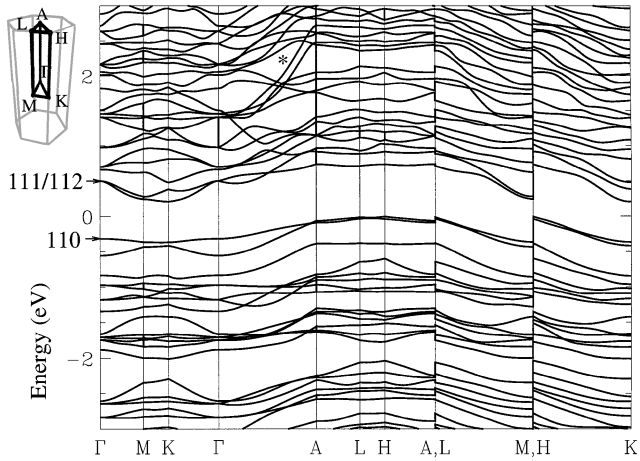

FIG. 2. Band structure of (Na,Se) in the hexagonal BZ. The BZ is indicated on the left. Three bands are labeled by their numbers in energetic order at $\vec{k}$ point Γ, and a star is used to denote two dispersive bands; see text.

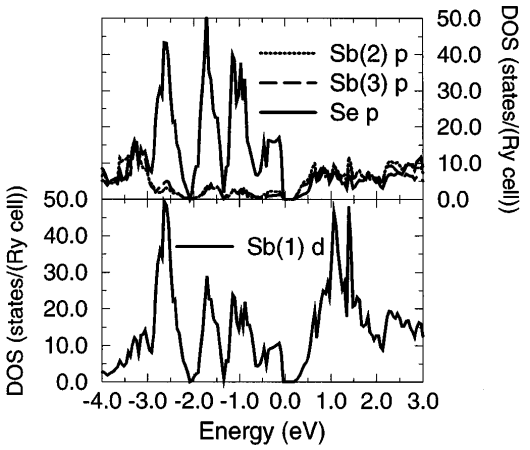

FIG. 3. Angular momentum-projected densities of states of the (Na;Se) compound around the Fermi energy for the dominant orbitals.

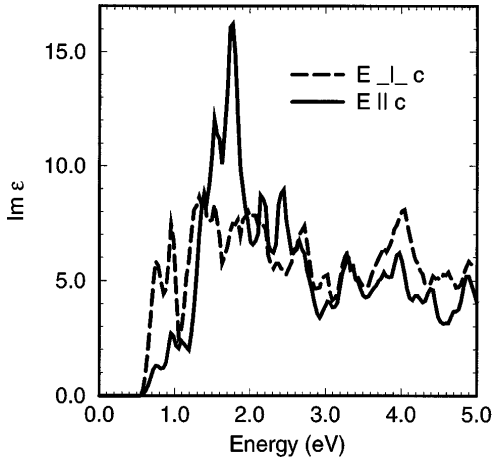

FIG. 4. Imaginary part of the dielectric function ε of (Na;Se) for $\vec{E}$ parallel and perpendicular to the c axis.

of trivalent Sb III. Their overall contribution becomes, mainly as p states, significant above the gap. The d states of the wall Sb atoms give an almost vanishing contribution within the first 4 eV ranges below and above the gap. The chalcogen X atoms are essentially of p character and dominate, together with the d states of Sb(1), the bound part of this energy range. The valence band maximum appears at the H point and the conduction band minimum 0.2 eV above at the K point. The direct gap of slightly more than 0.5 eV occurs at the K point. The uppermost occupied band (No. 110, see Fig. 2) belongs to the identical representation of the group C_3 generated by a 120° rotation along the c axis at Γ. The degenerate lowest conduction band (Nos. 111/112) contains two one-dimensional representations which split outside Γ. Going to A, on the top of the Brillouin zone, both bands cross yielding for the lower (upper) one the one-dimensional representation which transforms in multiplying by the phase factor $e^{2\pi i/3}$ for a counterclockwise (clockwise) rotation. In (Na;Se), apart from a fundamental indirect gap, a second gap appears around -2 eV. In the remaining three compounds this gap is bridged by a low DOS. Separate calculations for a crystal with only the tube walls included and for one which contained only the outer $[SbX_3]^{3-}$ pyramid chains and the inner sodium atoms have been done.

For the latter the fundamental gap almost closes leaving a small DOS at the Fermi level. For the former this gap is still existing but significantly reduced. Together with an increasing dispersion and increasing similarity in the energetic distribution of the aforementioned binding orbitals in going to the full crystal, it shows the intimate connection of both building units, the walls, and the outer pyramid chains. Not these units separately but only the full system exhibits a stable crystal. The outer pyramids seem to contribute the electronic glue to bond the tubes widening their gap to the final amount. The alkali s state remains almost entirely depopulated in all cases.

Figure 4 displays a high maximum in the calculated imaginary part of ε, which is a typical feature for all four compounds. Differing compositions $(A;X)$ mainly cause a shift of the onset and the high maximum as described below. A remarkable change with polarization appears in the close neighborhood of the onset of optical absorption and, with an opposite sign, around the main absorption peak. The polarization with $\vec{E}$ parallel to the c axis leads to an absorption smaller in slope by a factor of 4 near the onset compared with the perpendicular case. As the onset is associated with the K point, the reduction for the parallel polarization is attributed to the selection rule induced by C_3 which should suppress transitions between the symmetric valence band and both lower conduction bands having less symmetry. Because temperature dependent measurements of the conductivity are still lacking, the details of the thermally activated conductivity are open to question. However, the lowest conduction band shows a maximum dispersion of 0.5 eV along KH (see Nos. 111 and 112, respectively, in Fig. 2), larger by a factor of 2 compared with KΓ, indicating an anisotropic conductivity enhanced along the c direction in the absence of impurities. A strong hybridization of the Sb(1) d and X p orbitals of the outer $[SbX_3]^{3-}$ pyramids with the Sb(2) p orbitals of the $[SbO_3]$ pyramids of the wall is observed within the lower 4 eV of the conduction bands (Fig. 3). This suggests a mechanism for the conductivity which involves the electron transfer between the two types of pyramids. Within the lowest conduction bands the Sb(1) d orbitals of xz and yz type dominate in conjunction with Sb(2) and Sb(3) p orbitals of x and y type, where the z axis is aligned to c.

Figure 5 displays the chemical trend of calculated band gaps of the four members of the cetineite family. As usual in local density theory the gaps might be underestimated. Especially, the high degree of localization in bands around the gap presumably widens the gap by enhanced exchange. Also the exact onset of both absorption and photoconductivity is difficult to derive from the experimental data obtained at room temperature. We believe that one should rather consider the direct transition energy

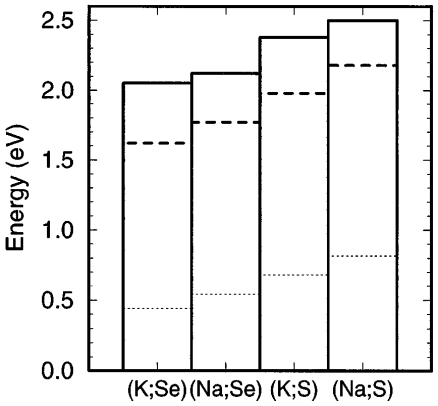

FIG. 5. Experimental optical gaps (solid line) [12,16] and theoretical energies of maximum absorption (dashed line) together with the direct band gaps (thin dotted line) dependent on the composition of the crystal.

corresponding to the high maximum in the imaginary part of the dielectric function to account for the absolute values of the onsets.

Disregarding this uncertainty in the interpretation of the absolute values the chemical trend itself shows excellent agreement with the experimental results. It follows the ionization energy of the alkali atoms which is larger for sodium than potassium, thus enhancing the binding energy and thereby the gap for sodium. This is to be expected as the valence shell of these atoms is completely ionized in all four compounds studied. The larger gaps of the sulfur compounds as compared with the selenium ones confirm the trend which is met in many covalently bound crystals containing these elements, as e.g., the II-VI or III-VI compounds, and reflects most probably the strength of the SbX_3 binding in the outer pyramids.

Current investigations concern a possible correlation between the trend for the alkali atoms and the bond angle in the $[SbX_3]^{3-}$ pyramids among the sulfur and selenium compounds, respectively, in continuation of the work by Wang and Liebau [17].

The observed photoconductivity [12,16] shows that a significant electronic population of the conduction bands is induced by irradiation. The frequency dependence of the photoconductivity near the onset follows that of the optical absorption. The measured onset should be associated with the high absorption part of ε and not with the lowest conduction band. At that energy, bands with much higher dispersion are available for the excited conduction electrons, especially in the ΓA direction. Two bands, for example, (see $*$ in Fig. 2) disperse from 1.4 to 2.6 eV (dominated by all Sb(1) d orbitals except the z^2 type). A photoconductivity, anisotropic as well but significantly enhanced over the thermally activated conductivity, is the consequence. It is experimentally observed as roughly 10^2 of the dark conductivity. A crucial experiment to decide on how to position the theoretical bands would be the measurement of the anisotropy of both the conductivity and the optical absorption. Instead of a final answer this part of the discussion rather shows for this exciting new material the problems which have to be solved after the first theoretical access.

To summarize, we have self-consistently calculated the electronic structure and optical properties of a most promising family of nanoporous compounds. It proves that such calculations are not only feasible but offer essential physical insight into the correlation between the geometry and chemical character of the bonds on one hand, and the electronic structure on the other. A remarkable difference of more than 1 eV between the calculated fundamental band gap and the calculated pronounced maxima of absorption appears. The latter coincide in energy with the observed onsets of photoconductivity and absorption suggesting that the measurements at room temperature display the pronounced features of the dielectric function not resolving the fundamental gap. The experimentally found chemical trend within a series of four compounds could be theoretically reproduced and explained. This finding does not depend on whether the size of the fundamental gap or the position of maximum absorption is regarded.

This work was supported by the "Bundesministerium für Bildung, Wissenschaft, Forschung umd Technologie" under Contract No. 05 605 FKA1 and by the "Deutsche Forschungsgemeinschaft" under Contract No. SI 609/2-1.

[1] *Clusters and Colloids*, edited by G. Schmid (VCH, Weinheim, 1994).
[2] H. Weller, Angew. Chem. **105**, 264 (1996); Angew. Chem. Int. Ed. Engl. **32**, 250 (1993).
[3] A. P. Alivisatos, J. Phys. Chem. **100**, 13 226 (1996).
[4] G. Schön and U. Simon, Colloid Polym. Sci. **273**, 101 (1995); *ibid.* **273**, 202 (1995).
[5] T. Sato, H. Ahmed, D. Brown, and B. F. G. Johnson, J. Appl. Phys. **82**, 696 (1997).
[6] C. B. Murray, C. R. Kagan, and M. G. Bawendi, Science **270**, 1336 (1996).
[7] A. Doron, E. Katz, and I. Willner, Langmuir **11**, 1313 (1995).
[8] G. A. Ozin, Adv. Mater. **4**, 612 (1992).
[9] M. Reed, Sci. Am. **268**, No. (1), 98 (1993).
[10] F. Liebau and X. Wang, Beih. Eur. J. Mineral. **7**, 152 (1995).
[11] X. Wang, Z. Kristallogr. **210**, 693 (1995).
[12] U. Simon, F. Schüth, S. Schunk, X. Wang, and F. Liebau, Angew. Chem. **109**, 1138 (1997); Angew. Chem. Int. Ed. Engl. **36**, 1121 (1997).
[13] A. Trave, F. Buda, and A. Fasolino, Phys. Rev. Lett. **77**, 5405 (1996).
[14] O. K. Andersen, Phys. Rev. B **12**, 3060 (1975).
[15] X. Wang, Ph.D. Thesis, University of Kiel, Germany, 1993; X. Wang and F. Liebau (unpublished).
[16] J. Jockel, H. Wiggers, S. Schunk, and U. Simon (to be published).
[17] X. Wang and F. Liebau, Acta Crystallogr. Sect. B **52**, 7 (1996).